Check for updates

ADVANCED FUNCTIONAL MATERIALS
www.afm-journal.de

Design, Fabrication, and Screening of Environmental-Thermal Barrier Coatings Prepared by Ultrafast High-Temperature Sintering

Hua Xie, Victor K. Champagne III, Wei Zhong, Bryson Clifford, Shufeng Liu, Liangbing Hu, Ji-Cheng Zhao,* and David R. Clarke**

The demand for more efficient gas turbines relies heavily on the development of new environmental-thermal barrier coatings (ETBCs). However, there is still uncertainty about which alloys and composites will be used for the next generation of turbine blades, as well as the most promising coating materials. Herein, an ETBCs development strategy is presented by integrating the coating design, synthesis, and screening using an ultrafast high temperature sintering (UHS) technique to accelerate coating improvements. The initial basis for composition selection is their thermal expansion mismatch with the substrate alloys; for which a temperature-dependent coefficient of thermal expansion database is created. By combining tape casting method with the UHS technique a high-throughput synthesis of single and multi-layer coatings are realized with different compositions, layer stacking sequences, and layer thicknesses. To evaluate the coatings, thermal cycling tests from room temperature to 1300 °C are conducted. The approach enabled coatings on objects with complex geometries, multi-layer ETBCs, and porosity tailoring by using staged UHS that runs with different temperatures and durations. The fast iteration strategy is more cost-effective for the screening of ETBCs compared to conventional methods and greater throughput which can be further extended for rapid optimization of other materials systems.

1. Introduction

There is a pressing need for the development of new environmental-thermal barrier coatings (ETBCs) that can protect components in gas turbines and jet engines at temperatures above 1700 °C for greater efficiency.[1] However, there are still challenges preventing the rapid development of new coating compositions and multilayer structures for advanced environmental and thermal protection of alloys, both refractory metal and advanced ceramic matrix composites. A major bottleneck is the long time and high cost in screening new material compositions and applying them as coatings. Conventional methods such as atmospheric plasma spray (APS) require large amounts of powders (within a particular particle size range) to be made of each coating composition, which is immaterial for the production of the final parts but is disadvantageous for the rapid development of new coatings. For electron-beam physical vapor deposition (EB-PVD), large differences in vapor pressures of the component elements make it difficult to choose suitable coating compositions from the potential candidates.[1,2] Additionally, mapping the process parameters is a substantial, time-consuming effort to achieve the desired coating microstructures and density for each composition. Making multilayer coatings by these methods requires considerable development, and in the case of EB-PVD, needs multiple hearths and the ability for "beam jumping".[3] More efficient approaches are still needed to accelerate coating composition selection and evaluation.

In this study, we introduce an ultrafast, high temperature sintering (UHS) method[4] to accelerate the ETBC investigation process (**Figure 1**a). The heating process is primarily by thermal radiation. The advantages of UHS include an ability to reach high-temperatures (in excess of 2000 °C) in seconds so that densification occurs primarily by bulk-diffusion and the competing processes such as grain coarsening and pore growth are minimized. The sintering time is consequently shorter, thereby minimizing undesirable phenomena, such as abnormal grain growth and volatilization of some components. Additionally, rapid coating densification can be achieved without significantly raising the temperature of the underlying substrate material so coatings can be formed without adversely affecting the substrate material. We have built a coefficient of thermal expansion (CTE) database of potential alloy and composite substrates and coating materials to

H. Xie, W. Zhong, B. Clifford, S. Liu, L. Hu, J.-C. Zhao
Department of Materials Science and Engineering
University of Maryland
College Park, MD 20742, USA
E-mail: binghu@umd.edu; jczhao@umd.edu
V. K. Champagne III, D. R. Clarke
John A. Paulson School of Engineering and Applied Sciences
Harvard University
Cambridge, MA 02134, USA
E-mail: clarke@seas.harvard.edu
L. Hu
Center for Materials Innovation
University of Maryland
College Park, MD 20742, USA
The ORCID identification number(s) for the author(s) of this article can be found under https://doi.org/10.1002/adfm.202309978

DOI: 10.1002/adfm.202309978

 © 2023 Wiley-VCH GmbH

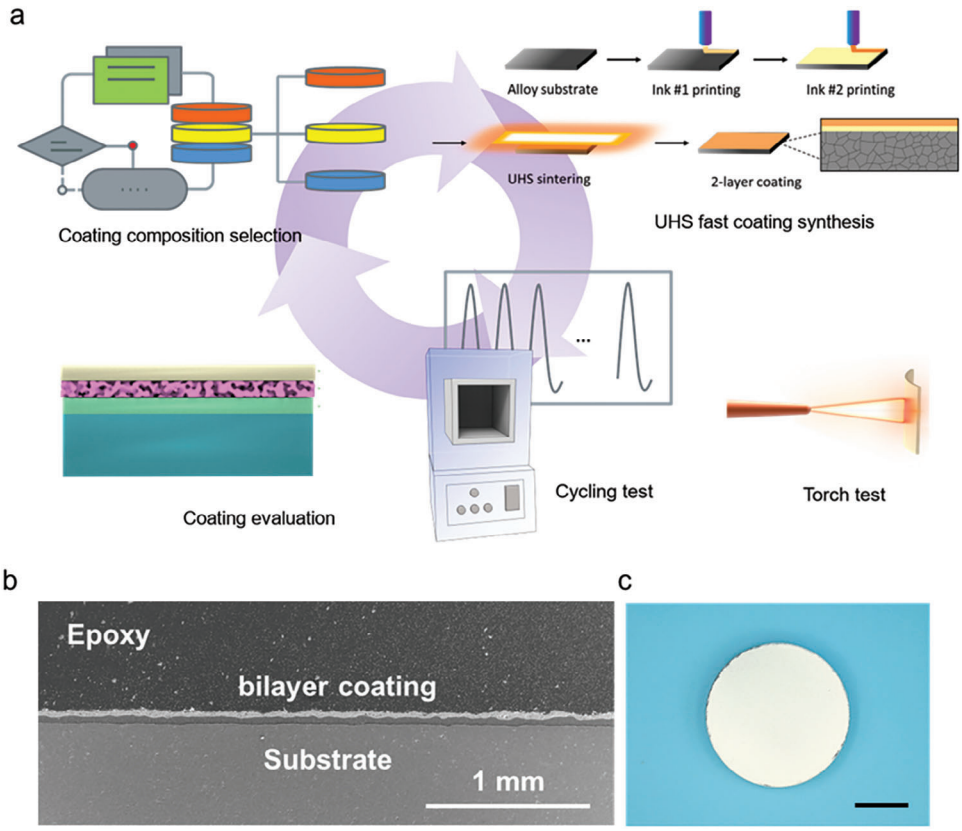

Figure 1. The overall strategy of using UHS as a new method for ETBCs investigation. a) Schematic showing the process of coating investigation using UHS: Potential coating selection, coating fast synthesis using UHS and coating performance test processes. b) A cross-sectional SEM image showing a bilayer BSAS-alumina coating structure on a polycrystalline SiC substrate. c) Photo showing top view of the 1-inch button with the coatings after the UHS treatment, which remains intact on the substrate.

guide the coating composition selection together with other considerations such as melting points, thermal stability, compatibility, as well as high-temperature mechanical properties. This not only enables a much larger repertoire of compositional variables and combinations to be assessed qualitatively but, just as important, determines ones that fail so that no further effort needs to be expended on them. Together with approaches to produce layers of powders, such as ink spraying, tape casting, or slurry dip technique, UHS is used to sinter the powders to create intact coatings on a variety of substrate materials in a short time. Subsequently, the coated substrates are subjected to high-temperature thermal cycling in air or exposure to a high-velocity torch test as the first steps to evaluate the coatings' stability and performance in protecting the substrates from degradation. Based on the feedback of the test data, coating compositions, and thicknesses are adjusted to improve the performance, and down-selected compositions and multilayers that pass the qualitative assessment can then be studied in successively greater detail. For instance, Figure 1b is the cross-sectional scanning electron microscopic (SEM) image of a bilayer barium strontium aluminosilicate (BSAS)-alumina coating on a polycrystalline SiC substrate. The bilayer coating is intact on the 1-inch coupon substrate after the UHS process, as shown in Figure 1c. We have also demonstrated other coatings and combinations on various substrates with the UHS approach (shown in Figures S1–S4, Supporting Information), which presents excellent universality in the sintering process to meet the requirements of coating/substrate selections for either single layer or multilayer coatings with different structure design. The UHS approach has further shown its flexibility for coating depositions on objects with complex geometries, two-phase coatings for CTE adjustments, as well as periodic, multilayer coating design. Our fast iteration strategy can be more cost-effective for the screening of ETBCs compared to current methods on account of lower capital costs and much higher throughput. The same strategy can be used for other materials system optimization such as producing high melting point multicomponent refractory alloys.

2. ETBC Design Considerations

New compositions for ETBCs must be based on materials with high melting points (e.g., ≥ 1800 °C), thermal stability and compatibility, low thermal conductivity, and a low CTE mismatch with the ultrahigh temperature alloy substrate or SiC-based composites. Additionally, multiple layers of coating materials that can be used as ETBCs may be needed to confer different functionalities such as minimizing high-velocity steam recession rate, CTE mismatch, and thermal conductivity. Our coating design aims to satisfy two overriding requirements. The first is minimizing the probability that it mechanically spalls or delaminates on cooling. This is the so-called "prime reliance"

© 2023 Wiley-VCH GmbH

16163028, 0, Downloaded from https://onlinelibrary.wiley.com/doi/10.1002/adfm.202309978 by Harvard University, Wiley Online Library on [01/12/2023]. See the Terms and Conditions (https://onlinelibrary.wiley.com/terms-and-conditions) on Wiley Online Library for rules of use; OA articles are governed by the applicable Creative Commons License

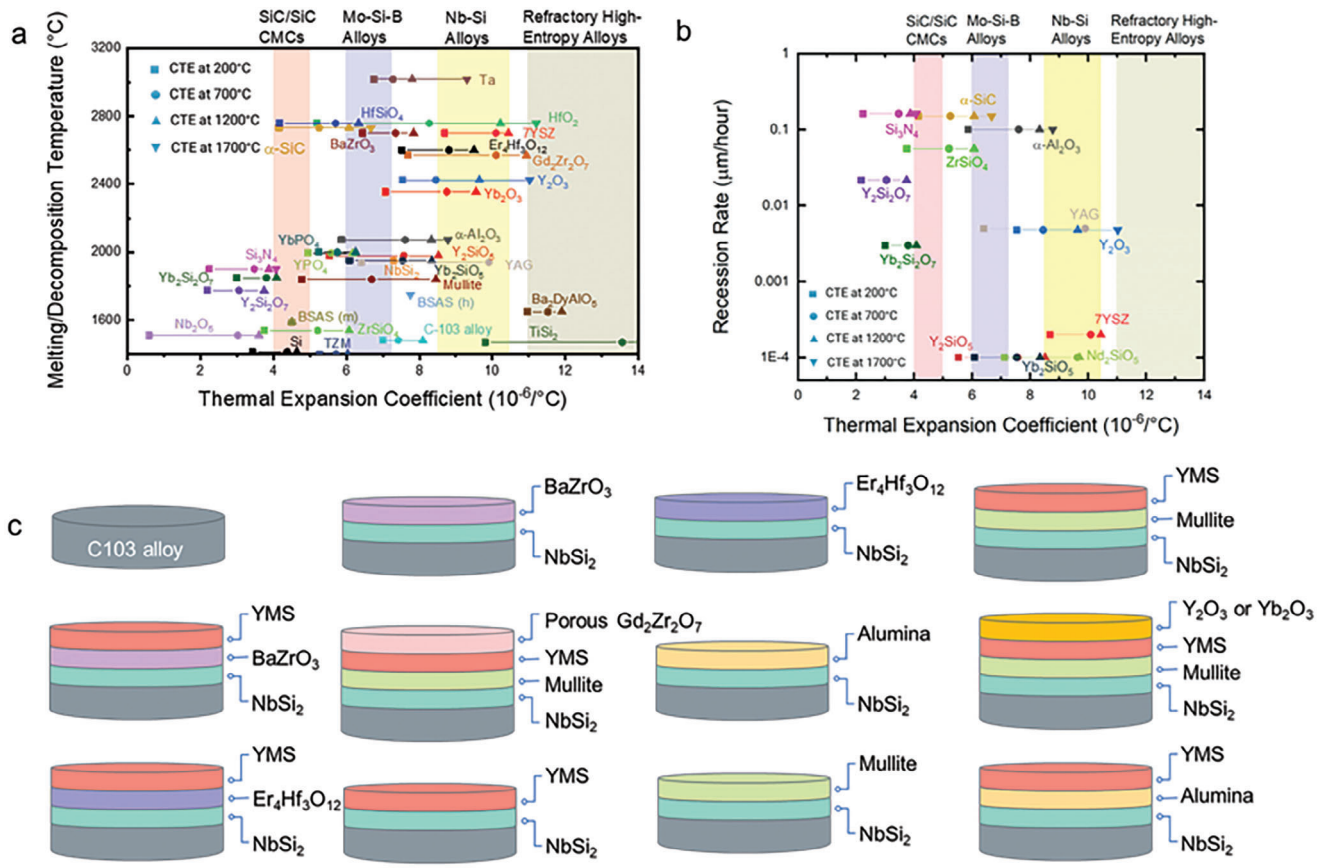

Figure 2. Coating candidate material analysis and design. a) The CTE matching for various coating and substrate compositions considering the phase stabilities. As the thermal expansion coefficients are a function of temperature, their values at specific temperatures are indicated by the symbols along the line. b) Recession rate in a high-velocity steam environment versus thermal expansion coefficient adapted from.[14] The thermal expansion coefficient data in Figure 2a,b are from.[16–36] c) Some candidate coating compositions for C-103 Nb-based substrate.

criterion and requires minimizing the overall strain energy associated with CTE mismatch with the substrate. The second is that the coatings and the substrate are phase compatible, i.e., do not chemically react at the very highest operating temperatures.

Large CTE mismatches can result in coating delamination or cracking during thermal cycling due to the build-up of elastic strain energy associated with thermal stresses. The strain energy release rate, G, driving mechanical failure is proportional to the square of the mismatch strain: for a multilayer coating, the strain energy release rate is given by the sum of the strain energy release rates of each of the N layers[5,6]:

$$G = \frac{(1-\nu^2)}{2} \sum_{n=1}^{N} h_n \int_{T0}^{T1} \left(\Delta\alpha_n \, \Delta T\right)^2 E_n(T) \, dT \quad (1)$$

where υ is Poisson's ratio, h_n is the thickness of the n-th layer, T_0 and T_1 are the initial and final temperatures, $\Delta\alpha_n$ is the difference between the thermal expansion coefficients, and E_n is the Young's modulus of the n-th layer. Delamination only occurs if the strain energy release rate exceeds the interfacial toughness, Γ. (Generally, this value is not known). To identify coating materials for minimal thermal expansion mismatch, we have built a database from the literature of CTE versus temperature data for a variety of substrate and coating candidates.

Consequently, different coating material combinations will be required for different ultrahigh-temperature alloy or composite substrate families. Additionally, the CTE of rare-earth (RE) oxides, monosilicates, disilicates, zirconates, systematically varied by cation substitution for instance, by altering the concentration of different rare-earth ions in rare-earth oxides, for instance, partially or completely replacing Y by Yb in yttrium monosilicate (Y_2SiO_5, YMS). This is a degree of compositional design that is extremely time-consuming (and expensive) by traditional sintering and deposition processing routes but becomes feasible using UHS.

To better compare the CTEs of various coating materials and those of the potential substrates and to take the phase stability into consideration, we have represented the CTE data on a plot of melting/decomposition temperatures for potential oxide compositions with different banners indicating potential substrate families, as shown in **Figure 2**a. Each horizontal line represents a different oxide, and the symbols represent the CTE values reported at different temperatures. To better elucidate the usage of the database, we here selected two representative substrate materials with different CTEs (i.e., polycrystalline SiC to represent the range of SiC composites with a very low CTE, and a commercial

© 2023 Wiley-VCH GmbH

16163028, 0, Downloaded from https://onlinelibrary.wiley.com/doi/10.1002/adfm.202309978 by Harvard University, Wiley Online Library on [01/12/2023]. See the Terms and Conditions (https://onlinelibrary.wiley.com/terms-and-conditions) on Wiley Online Library for rules of use; OA articles are governed by the applicable Creative Commons License

niobium alloy, C-103, containing Nb-Hf-Ti), for a more detailed coating match analyses.

New substrate materials including SiC ceramic-matrix composites (CMCs) have been developed for improved high-temperature mechanical properties and lower density. Other alloys are being developed for improved oxidation resistance, low creep rates, and higher temperature capabilities. The coatings candidates for the SiC substrate can be identified in Figure 2a with similar CTE values. Some of these coatings, including barium strontium aluminosilicate (BSAS), and mullite have been under development as EBTCs for SiC CMCs for several years.[7–9] These oxide compounds, and alumina were selected for UHS trials and their cumulative strains were plotted against SiC in Figure S5 (Supporting Information). The cumulative strain was calculated by computing the integral of the CTE versus temperature curve for each material.

Monoclinic BSAS has the smallest thermal strain mismatch to polycrystalline SiC, as shown by the cumulative strain curves almost overlaying, whereas the cumulative strain curves of hexagonal BSAS, alumina, and mullite diverge from that of SiC with increasing temperature differences. The coatings of hexagonal BSAS, alumina, and mullite will be under tension upon cooling since their cumulative strain curves lie above the SiC curve. The same procedure was undertaken for identifying potential coatings for the C103 niobium alloy, with a protective $NbSi_2$ bond coat. Yttrium oxide and yttrium monosilicate (YMS, Y_2SiO_5) were selected for further investigation, and their cumulative strain curves are plotted with the curves for C103 and $NbSi_2$ in Figure S6 (Supporting Information). The curve for yttrium oxide (Y_2O_3) lies above the curves for C103 and $NbSi_2$, so the coating will be under slight tension upon cooling. For comparison, the curve for YMS, lies below the curves for C103 and $NbSi_2$, so the coating will be under slight compression upon cooling. Yet both the Y_2O_3 and YMS curves almost overlay with the C103 and $NbSi_2$, which indicates a small thermal mismatch.

Additionally, for a coating to be considered viable for turbine applications, it also needs to survive in the high-velocity combustion gas in turbines. For example, SiC oxidizes in water vapor to form volatile CO (g), H_2 (g), and a silica scale.[10,11] Concurrently, volatilization of the silica formed occurs when it reacts with water vapor to form a silicon hydroxide gas, $Si(OH)_4$ (g). Because of these reactions, silicon in silicon-containing materials exposed to water vapor is depleted over time, starting at the surface of the material. Similarly, Al_2O_3 reacts with water vapor to form a volatile aluminum hydroxide species. As the partial pressure of water vapor increases, the partial pressure of aluminum hydroxide also increases, causing a rapid loss of coating mass, commonly represented by a recession rate.[12] Figure 2b summarizes a large body of literature concerning high-velocity steam recession rates of materials, measured at 1450 °C as a function of CTE. Some materials that show the lowest recession rates include the RE monosilicates (Yb_2SiO_5, Y_2SiO_5, and Nd_2SiO_5), yttrium aluminum monoclinic (YAM, $Y_4Al_2O_9$), yttrium aluminum perovskite (YAP, $YAlO_3$), and yttria-partially stabilized zirconia 7YSZ.[13,14]

Figure 2c illustrates several potential multilayer coating materials on a C103 substrate after matching their properties. Amongst the most promising is the YMS-$NbSi_2$-C103 combination. Besides the CTE matching and high-temperature phase stability, other coating concepts and incorporating porosity to decrease thermal conductivity and elastic modulus can also be considered. Since no fully dense oxide has a thermal conductivity <1 W m^{-2} at $\geq$1000 °C, in accordance with physical models for minimum thermal conductivity,[15] decreases in thermal conductivity can only be achieved by incorporating porosity, essentially decreasing the effective cross-sectional area through which phonons can propagate.

3. ETBC for the C-103 Nb Alloy

Based on the analyses above, we selected YMS/$NbSi_2$ coatings on the C-103 substrate to demonstrate the UHS process as proof of concept. A $NbSi_2$ bond coat, an essential coating to prevent catastrophic oxidation of niobium, was first deposited via a pack cementation method. To improve the ETBC coating uniformity, we employed the tape cast method to deposit the YMS topcoat, in which YMS powders were mixed with binder and plasticizer (benzyl butyl phthalate and polyvinyl butyral), dispersed in toluene, and coated on the coupons, followed by a pre-heat treatment at 450 °C for 20 min for the binder removal. **Figure 3**a schematically shows the UHS process for the C-103 coupons with coatings, in which the carbon felt strip heater was set ≈1 mm above the coating surface and the heating profile was program-controlled to confirm stable power output (Figure 3b). A two-camera temperature measurement system was employed to measure and calibrate the UHS heating temperature (Figure S7, Supporting Information), and the sintering parameter was set at ≈1900 °C for 2 min. Figure 3c presents the polished cross-sectional SEM image of the YMS/$NbSi_2$ coatings on the C-103 substrate after the UHS treatment. The YMS topcoat was intact and adhered to the bond coat without any vertical cracks, further confirming the excellent CTE match among the topcoat, bond coat, and the C-103 substrate, consistent with the CTE mismatch analysis above. The EDS line scan results (Figure 3d) further indicate a clear element distribution distinction between the topcoat and bond coat, corroborating that the two coatings are well compatible with each other and do not show any reaction even at the high temperature during sintering.

4. Thermal Cycling Testing

After a coating meets the requirement that it remains adhered to the substrate after UHS processing and does not shrink or expand laterally relative to the substrate (to achieve complete coverage) after the UHS process, it is a candidate for the next requirement, thermal cycling. This test is an important criterion for selection as a viable coating/substrate combination because ETBCs must undergo hundreds of heating and cooling cycles in use in a gas turbine engine. To evaluate the YMS/$NbSi_2$ coatings on the C-103 coupon after the UHS processing, they were thermally cycled from room temperature to 1300 °C, in a program-controlled thermal cycling system, as schematically shown in **Figure 4**a. The thermal cycling test apparatus is further shown in Figure 4b and consists of a 1500 °C capable tube furnace, alumina rods that are driven in and out of the furnace by a stepper motor, a thermocouple underneath the test coupon (Figure 4c), which is mounted on alumina rails enabling rapid heating and cooling rates as both

© 2023 Wiley-VCH GmbH

16163028, 0, Downloaded from https://onlinelibrary.wiley.com/doi/10.1002/adfm.202309978 by Harvard University, Wiley Online Library on [01/12/2023]. See the Terms and Conditions (https://onlinelibrary.wiley.com/terms-and-conditions) on Wiley Online Library for rules of use; OA articles are governed by the applicable Creative Commons License

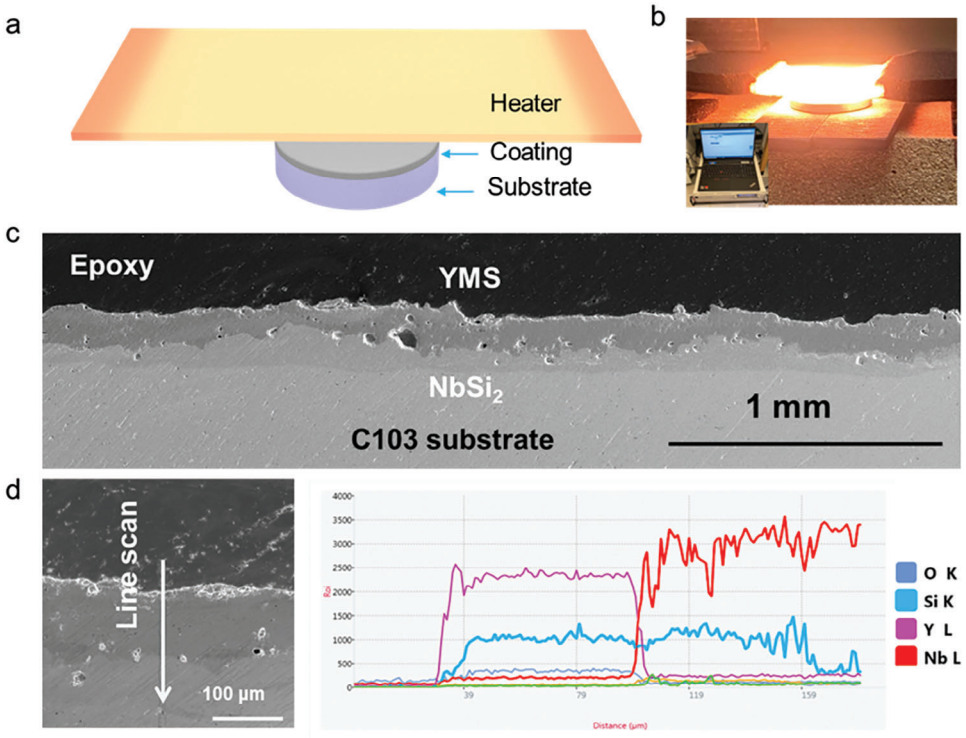

Figure 3. Characterization of the UHS-applied coatings on the C-103 substrate. a) Schematic of the coating sintering process with UHS. b) Photo showing the UHS process for sintering the coating. The inset photo shows the programmable UHS parameters adjusted by the output voltage and current. c) The polished cross-sectional SEM image of the YMS-$NbSi_2$ coatings on the C-103 substrate, in which the topcoat and bond coat show a well-defined interface. d) EDS line scan for the cross-sections of the YMS-$NbSi_2$ coatings on the C-103 substrate, clearly delineating the element distinction through the coating and into the substrate.

sides are exposed. The entire process is automated under Python controlled software. A thermal cycle consists of heating the test coupon in the furnace for 30 minutes, then allowing it to cool for 25 min outside of the furnace (Figure 4d,e) and recording an image of the sample after each cycle. The heating and cooling rates were 550 and 480 °C min^{-1}, respectively. Using this test protocol, the time, temperature, and number of cycles can be controlled while identifying at which cycle the coating begins to spall with the time-stamped images.

Figure 4f shows a photo of the YMS/$NbSi_2$-C103 coupons before and after testing for 50 cycles. The coating successfully survived the 1300 °C thermal cycling test without any coating spallation. We further conducted tensile tests of the YMS/$NbSi_2$-C103 dog bone sample after a high-temperature treatment at 1400 °C for 20 h and compared them with the samples that had not been coated (Figure S8, Supporting Information). The samples showed similar ductility with a tensile strain ≈40%, showing no adverse effect due to the transient heating during the short but very high-temperature exposure associated with the UHS process, or from any oxygen embrittlement due to oxygen ingress into the C-103 alloy.

5. UHS for Complex Geometries

We also employed UHS for coating objects with complex geometries, for instance, the airfoil shape, shown in **Figure 5**a. This was accomplished by wrapping a flexible carbon strip around the 3D shape to achieve conformal sintering. The turbine blade shapes were made from Nb tubes with 1-inch diameters (Figure S9, Supporting Information) to demonstrate the capability of the coating process. After UHS processing, the coatings were conformal and uniform.

The UHS process can also incorporate porosity by lowering the sintering temperature or using a shorter sintering time, with the degree of porosity being determined by varying the sintering time and temperature. In this way, we have synthesized bilayer and multilayer coatings with different porosities by a two-step process. This also has the potential to tune both the thermal conductivity and elastic modulus by adjusting the porosity of the coatings. To do this, we mixed colloidal polystyrene particles into powder slurries of the coating composition, dried the coating, and burnt out the polymer binder at low temperatures. Then, the UHS heating was rapidly increased to achieve a high sintering rate to trap porosity within the coatings. We demonstrated one typical bilayer combination for the coating deposition on an alumina substrate, in which the YMS topcoat has a dense structure, and the intermediate mullite coating is porous (Figure 5b).

Additionally, we have demonstrated an ability to produce periodic multilayer coatings, which can be used to adjust the overall CTE mismatch with different substrates. In the example shown in Figure 5c, which consists of alternating layers of YSZ/α-alumina produced from periodic layered ceramic powder tapes. In the SEM images, the two different layers can be readily distinguished on account of their atomic number contrast. The

© 2023 Wiley-VCH GmbH

16163028, 0, Downloaded from https://onlinelibrary.wiley.com/doi/10.1002/adfm.202309978 by Harvard University, Wiley Online Library on [01/12/2023]. See the Terms and Conditions (https://onlinelibrary.wiley.com/terms-and-conditions) on Wiley Online Library for rules of use; OA articles are governed by the applicable Creative Commons License

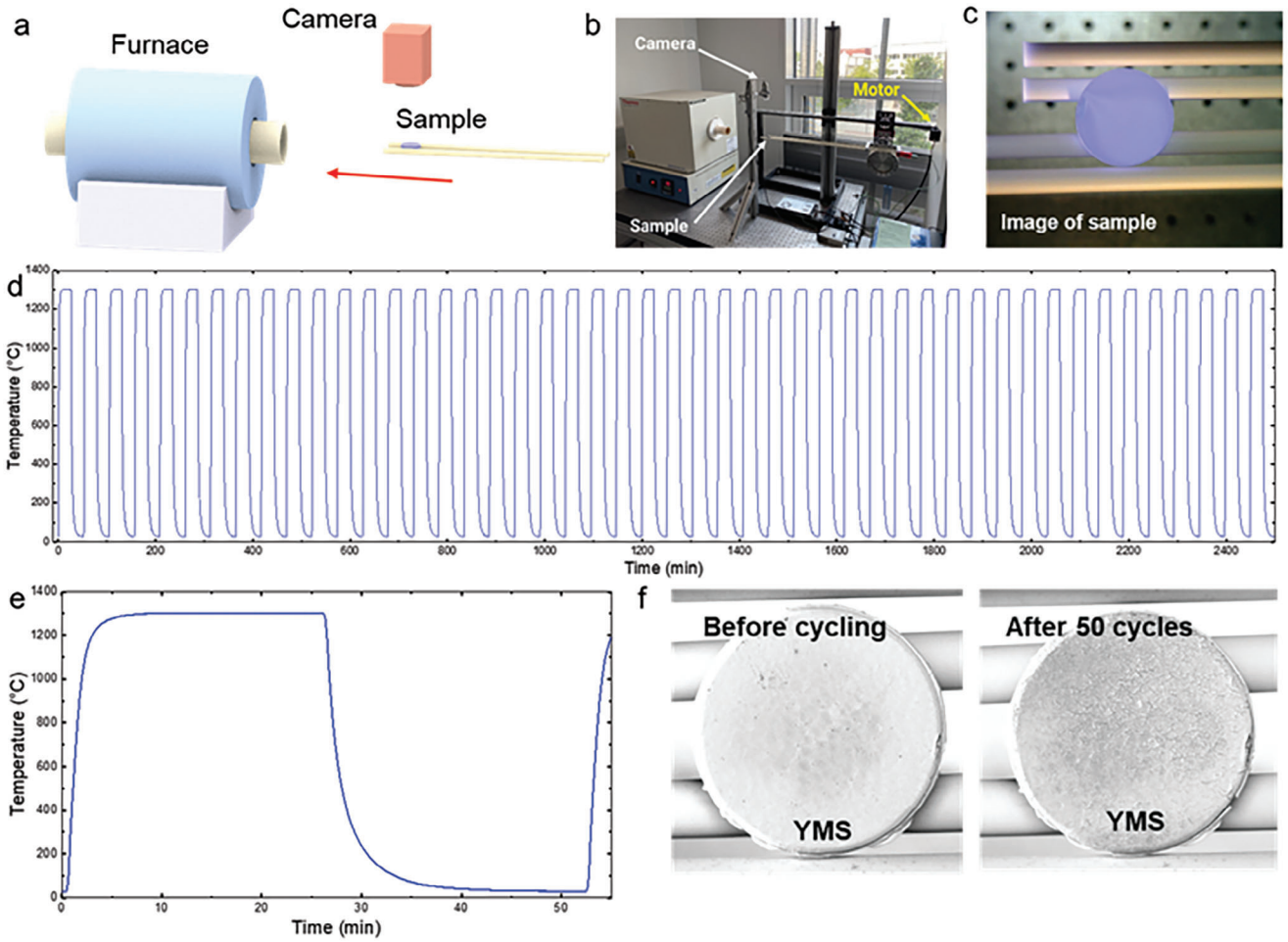

Figure 4. The thermal cycling testing of coatings. Thermal cycling test setup schematic a) and photograph b). c) A one-inch diameter coupon sample resting on alumina rods for cyclic testing. d) The cycling profiles at a furnace temperature of 1300 °C. e) The detailed cycling temperature profile for one cycle. f) Comparison of a Y_2SiO_5 coated, $NbSi_2$-bond-coated C103 niobium alloy button before and after 50 cycles, illustrating that the coating remains intact with only some slight edge spalling in the lower right.

YSZ/α-alumina is of particular interest as a high-temperature coating as these oxides are phase compatible to almost 1860 °C and consequently chemically stable to this temperature.[37] Furthermore, more traditional coating methods, such as EB-PVD, cannot deposit the thermodynamically stable α-alumina phase. Instead, the deposited alumina cracks as a result of the disruptive phase transformation as it converts to the stable alpha-phase when it is heated to high temperatures, typically above 1100 °C. By starting with α-alumina powders and sintering, there is no phase change and cracking is avoided. Additionally, we also UHS treated the YSZ/α-alumina mixtures at different temperatures (Figure S10, Supporting Information), and the clear phase distinction enables the adjustment of CTE by tailoring the composition ratios by varying their volume fraction in the future.

6. Conclusion

We have demonstrated an approach for the rapid development of environmental-thermal barrier coatings by employing an ultrafast high temperature sintering (UHS) technique to accelerate the iterations of the design, selection, deposition, and evaluation of coating compositions. A CTE database was built based on literature experimental data, from which suitable coating materials were selected for specific ultrahigh-temperature alloy or composite substrate families with minimal CTE mismatch.

We combined tape casting with the UHS technique to realize high-throughput and cost-effective screening of compositions and rapid fabrication of new coatings, which overcomes the difficulties of coating compositional design that is extremely time-consuming (and expensive) by traditional sintering and deposition processing routes but becomes feasible using UHS. The UHS technique has the capability to reach very high temperatures in seconds so that densification occurs rapidly by bulk diffusion, which can minimize undesirable grain growth and preferential volatilization of some components. Additionally, coating densification can be achieved without significantly raising the temperature of the underlying substrate materials so coatings can be formed without adversely affecting the substrate materials.

© 2023 Wiley-VCH GmbH

16163028, 0, Downloaded from https://onlinelibrary.wiley.com/doi/10.1002/adfm.202309978 by Harvard University, Wiley Online Library on [01/12/2023]. See the Terms and Conditions (https://onlinelibrary.wiley.com/terms-and-conditions) on Wiley Online Library for rules of use; OA articles are governed by the applicable Creative Commons License

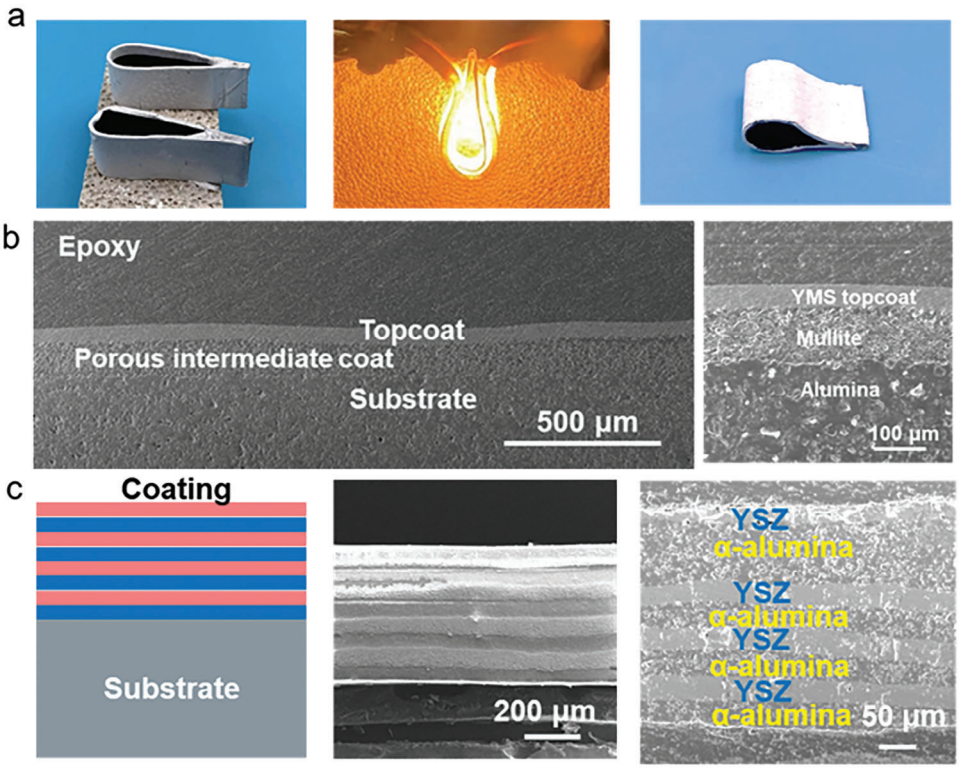

Figure 5. Coating complex shapes. a) A 3D turbine blade shape made from Nb tubes, a photo of the UHS coating sintering process and the airfoil-shaped tube after coating. b) The coating design with a topcoat of dense YMS coating and an intermediate porous mullite coating on a polycrystalline alumina substrate. The SEM image of the coating at a higher magnification. c) A periodic multilayer coating design with repeated YSZ and α-alumina layers.

Single layer synthesis was performed to optimize the UHS temperature and time for various density levels. Multilayer ETBCs were further synthesized via UHS with high throughputs and the porosity in different layers was tailored with suitable UHS temperatures and durations. Thermal cycling tests of these coatings were conducted from room temperature to 1300 °C: coatings that remained intact after 50 cycles can be further evaluated to improve process parameters for longer lifetimes.

We also employed the UHS approach to realize coatings on objects with complex geometries, periodic multilayer ETBCs, as well as porosity tailoring for different layers. Our strategy can be used to develop higher temperature-capable coatings that will meet or exceed the ever-increasing performance requirements of gas turbines and shed light on the fast synthesis of coatings that are applicable to broader applications.

7. Experimental Section

Thermal Expansion Database: The coefficient of thermal expansion versus temperature data was acquired from several sources in the literature. For data sets that were plotted, a plot digitizer was used to acquire the individual data points. To compare the CTEs of potential single or multilayer coatings, the integrated CTE referred to as the "cumulative strain" versus temperature was plotted against the turbine blade substrate material. The difference in the cumulative strain between materials should be minimized to prevent delamination of the coating or coatings due to thermal expansion mismatch.

UHS Setup: The UHS system consists of a heating unit, a high current power supply, and temperature measurement unit all under computer control. The heater is a strip of carbon felt having typical dimensions of 50 mm × 150 mm × 5 mm. The two ends of the carbon felt were fixed on two graphite plates and an alumina plate was employed to fix the carbon felt graphite plates. The graphite plates also functioned as current collectors. A programmable supply system was used as the DC power source to elevate the temperature of the Joule heating components with a tunable current and voltage. A laptop was used to programmatically control the power output. The heating unit was located inside a glovebox filled with pure argon gas (Airgas, UHP300) at atmospheric pressure to control the gas atmosphere.

Temperature Measurement: The temperature of the UHS heater was determined using UV–vis spectra, captured through a custom-built system that utilized a Vision Research Phantom Miro M110 high-speed camera. This camera documented the heating process at an impressive speed of 1000 frames per second. The gray-body emissivity values of the carbon materials were incorporated into Planck's law. The normalized spectral signals were then derived based on the specifications provided by the camera manufacturer. For the calibration of the lower temperature region, an Infratec VarioCAM HD infrared camera was used.

Fabrication of the Tape Cast Membrane and Coatings: The coating powders (40 wt.%), toluene (45 wt.%), fish oil (0.5 wt.%) were weighed, mixed, and milled for 3 h. After the milling, benzyl butyl phthalate (8.5 wt.%) and polyvinyl butyral (6 wt.%) were added and milled for 6 h to form a slurry. The slurry was cast onto a polyethylene terephthalate (PET) sheet. The sheet was transferred to a vacuum oven and maintained for 6 h to get the membrane tape dry.

The Coating Synthesis Process: The membrane tape was transferred from the PET sheet and further attached on a C103 niobium alloy button substrate with $NbSi_2$ bond coat. The $NbSi_2$ bond coat was pre-sandblasted to increase the surface roughness. The button had a diameter of 1 inch

© 2023 Wiley-VCH GmbH

16163028, 0, Downloaded from https://onlinelibrary.wiley.com/doi/10.1002/adfm.202309978 by Harvard University, Wiley Online Library on [01/12/2023]. See the Terms and Conditions (https://onlinelibrary.wiley.com/terms-and-conditions) on Wiley Online Library for rules of use; OA articles are governed by the applicable Creative Commons License

(25.4 mm). The membrane tape coated substrate was first heated in a muffle furnace to burn off the polymer binders. The powder coated alloy was then transferred to the UHS system densified at temperatures up to the suitable temperature (usually 1700 – 2000 °C) for 1–2 min. The temperature measurement system was used to feedback and maintain the temperature during the whole process. The coating was rapidly densified and after it cooled down to room temperature, the button with densified YMS coating was transferred for further characterization.

Materials Characterization: The button with topcoat was mounted with epoxy resin and put in vacuum oven for 3 min at 60°C to get the resin completely cured. The mounted sample was ground with sandpapers with different grits to expose its cross-sections. The cross-sectional surface was further polished with alumina paste. The morphology of the coating/substrate was evaluated on a Tescan XEIA Plasma FIB/SEM. with EDS analysis at 15 kV. The tensile tests were conducted using an Instron 3365 universal testing system with a load capacity of 30 kN, at a cross-head speed of 2 mm min^{-1}.

Thermal Cycling Test: The thermal cycling test apparatus consisted of a tube furnace, with the test coupon sample lying on aluminum oxide rods that were driven in and out of the furnace by a computer-controlled stepper motor. A second set of alumina rods were attached to the drive and prevent the test button from moving as the rods were withdrawn. A thermocouple was mounted underneath the test coupon. The entire process was automated by running a Python program and in the test run, the furnace was set to 1300 °C. The program was set to heat the test button in the furnace for 30 min, then allow it to cool for 25 min outside of the furnace. The heating and cooling rates of the sample entering and leaving the furnace were 550 and 476 °C min^{-1}, respectively.

Supporting Information

Supporting Information is available from the Wiley Online Library or from the author.

Acknowledgements

The authors would like to acknowledge the support of ARPA-E grant DE-AR0001424. The authors acknowledge the support of the Maryland NanoCenter, its Surface Analysis Center and AIM Lab.

Conflict of Interest

The authors declare no conflict of interest.

Author Contributions

H.X. and V.C. contributed equally to this work. V.C. compiled the CTE database. D.C., J.Z., L.H., and H.X. designed the experiments. H.X., B.C., and S.L. carried out the coating synthesis and characterization experiments. V.C. and W.Z. conducted the coating evaluation experiments. All authors commented on the final manuscript.

Data Availability Statement

The data that support the findings of this study are available from the corresponding author upon reasonable request.

Keywords

coefficient of thermal expansion, environmental-thermal barrier coatings, high temperature refractory alloys, multilayer structures, ultrafast high-temperature sintering

Received: August 21, 2023
Revised: October 21, 2023
Published online:

[1] R. Darolia, *Int. Mater. Rev.* **2013**, *58*, 315.
[2] R. A. Miller, *Surface Coat. Technol.* **1987**, *30*, 1.
[3] U. Schulz, K. Fritscher, C. Leyens, *Surface Coat. Technol.* **2000**, *133*, 40.
[4] C. Wang, W. Ping, Q. Bai, H. Cui, R. Hensleigh, R. Wang, A. H. Brozena, Z. Xu, J. Dai, Y. Pei, C. Zheng, G. Pastel, J. Gao, X. Wang, H. Wang, J.-C. Zhao, B. Yang, X. (.R.). Zheng, J. Luo, Y. Mo, B. Dunn, L. Hu, *Science* **2020**, *368*, 521.
[5] J. W. Hutchinson, Z. Suo, *Adv. Appl. Mech.* **1991**, *29*, 63.
[6] M. R. Begley, J. W. Hutchinson, *The mechanics and reliability of films, multilayers and coatings*, Cambridge University Press, Cambridge, United Kingdom **2017**,
[7] K. N. Lee, R. A. Miller, N. S. Jacobson, *J. Am. Ceram. Soc.* **1995**, *78*, 705.
[8] K. N. Lee, *Surface Coat. Technol.* **2000**, *133*, 1.
[9] K. N. Lee, D. S. Fox, J. I. Eldridge, D. Zhu, R. C. Robinson, N. P. Bansal, R. A. Miller, *J. Am. Ceram. Soc.* **2003**, *86*, 1299.
[10] E. J. Opila, *J. Am. Ceram. Soc.* **2003**, *86*, 1238.
[11] N. S. Jacobson, *J. Am. Ceram. Soc.* **1993**, *76*, 3.
[12] P. J. Meschter, E. J. Opila, N. S. Jacobson, *Annu. Rev. Mater. Res.* **2013**, *43*, 559.
[13] M. Fritsch, H. Klemm, in *The Water-Vapour hot Gas Corrosion Behavior of Al2O3-Y2O3 Materials, Y2Si05 and Y3Al5O12-Coated Alumina in a Combustion Environment*, John Wiley & Sons, Inc, Hoboken, NJ, USA **2006**, pp. 148–159.
[14] C. Gatzen, D. E. Mack, O. Guillon, R. Vaßen, *Coatings* **2019**, *9*, 609.
[15] D. R. Clarke, *Surface Coatings Technol.* **2003**, *163–164*, 67.
[16] Y. S. Touloukian, et al., Thermophysical Properties of Matter - the TPRC Data Series. Volume 12. Thermal Expansion Metallic Elements and Alloys, **1975**,
[17] Y. S. Touloukian, T. Makita, Thermophysical Properties of Matter - the TPRC Data Series. Volume 13. Thermal Expansion - Nonmetallic Solids, **1977**,
[18] H. Wang, K. N. Lee, Coated article and method of making, U.S.P.a.T. Office, Editor. 2002: USA.
[19] M. Munro, *J. Am. Ceram. Soc.* **1997**, *80*, 1919.
[20] K. Fukuda, H. Matsubara, *J. Am. Ceram. Soc.* **2004**, *87*, 89.
[21] B. T. Richards, H. Zhao, H. N. G. Wadley, *J. Mater. Sci.* **2015**, *50*, 7939.
[22] M. Sokol, S. Kalabukhov, V. Kasiyan, A. Rothman, M. P. Dariel, N. Frage, *Optical mater.* **2014**, *38*, 204.
[23] K. Tsukuma, Y. Kubota, K. Nobugai, *J. Ceram. Assoc.* **1984**, *92*, 233.
[24] M. Ridley, J. Gaskins, P. Hopkins, E. Opila, *Acta Mater.* **2020**, *195*, 698.
[25] Z. Ding, M. Ridley, J. Deijkers, N. Liu, M. S. B. Hoque, J. Gaskins, M. Zebarjadi, P. E. Hopkins, H. Wadley, E. Opila, K. Esfarjani, *Materialia* **2020**, *12*, 100793.
[26] Y. Liu, W. Zhang, B. Wang, L. Sun, F. Li, Z. Xue, G. Zhou, B. Liu, H. Nian, *Ceram. Int.* **2018**, *44*, 16475.
[27] Z.-G. Liu, J.-H. Ouyang, Y. Zhou, J. Li, X.-L. Xia, *Int. J. Appl. Ceram. Technol.* **2009**, *6*, 485.
[28] J. Han, Y. Wang, R. Liu, F. Wan, *Scientific Rep.* **2020**, *10*, 13681.
[29] B. J. Harder, K. T. Faber, *Scr. Mater.* **2010**, *62*, 282.
[30] C. C. Wojcik, W. Chang, Thermomechanical processing and properties of niobium alloys, in International Symposium Niobium, **2001**,
[31] C. Wan, Z. Qu, Y. He, D. Luan, W. Pan, *Phys. Rev. Lett.* **2008**, *101*, 085901.
[32] I. Engström, B. Lönnberg, *J. Appl. Phys.* **1988**, *63*, 4476.

 © 2023 Wiley-VCH GmbH

16163028, 0, Downloaded from https://onlinelibrary.wiley.com/doi/10.1002/adfm.202309978 by Harvard University, Wiley Online Library on [01/12/2023]. See the Terms and Conditions (https://onlinelibrary.wiley.com/terms-and-conditions) on Wiley Online Library for rules of use; OA articles are governed by the applicable Creative Commons License

[33] D. Hancock, D. Homfray, M. Porton, I. Todd, B. Wynne, *J. Nucl. Mater.* **2018**, *512*, 169.
[34] L. F. Verkhorobin, N. N. Matyushenko, *Soviet Powder Metall. Metal Ceram.* **1964**, *2*, 468.
[35] R. Kassem, N. Al Nasiri, *Surface Coat. Technol.* **2021**, *426*, 127783.
[36] W. Hu, et al., *J. Mater. Sci. Technol.* **2019**, *35*, 2064.
[37] ACerS-NIST Phase Equilibria Diagram, CD-ROM Database, Version 3.0.

© 2023 Wiley-VCH GmbH

16163028, 0, Downloaded from https://onlinelibrary.wiley.com/doi/10.1002/adfm.202309978 by Harvard University, Wiley Online Library on [01/12/2023]. See the Terms and Conditions (https://onlinelibrary.wiley.com/terms-and-conditions) on Wiley Online Library for rules of use; OA articles are governed by the applicable Creative Commons License